THE JOURNAL OF PHYSICAL CHEMISTRY B

Article

pubs.acs.org/JPCB

Stacking Interactions between Adenines in Oxidized Oligonucleotides

Amedeo Capobianco,[†] Tonino Caruso,[†] Maurizio Celentano,[†] Anna Maria D'Ursi,[‡] Mario Scrima,[‡] and Andrea Peluso*,[†]

[†]Dipartimento di Chimica e Biologia and [‡]Dipartimento di Scienze Farmaceutiche e Biomediche, Università di Salerno, I-84084 Fisciano, Salerno, Italy

ABSTRACT: The effects of stacking interactions on the oxidation potentials of single strand oligonucleotides containing up to four consecutive adenines, alternated with thymines and cytosines in different sequences and ratios, have been determined by means of differential pulse voltammetry. Voltammetric measurements point toward the establishment in solution of structured oligonucleotide conformations, in which the nucleobases are well stacked altogether. Molecular dynamics simulations confirm that finding, indicating that single strands assume geometrical parameters characteristic of the B-DNA form. The analysis of the voltammetric signals in terms of a simple effective tight binding quantum model leads one to infer a robust set of parameters for treating hole transfer in one-electron-oxidized DNA containing adenines and thymines.

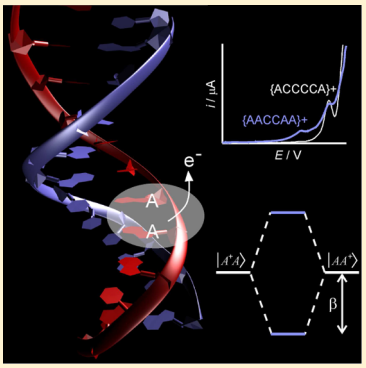

INTRODUCTION

Stacking interactions are of outstanding importance in the chemistry of DNA. Apart from being mainly responsible for the coiled conformations assumed by single strand or duplex in solution and in the solid state, they play a major role in DNA oxidation, both because they provide the necessary intrastrand nucleobase couplings for long-range hole transfer[1−7] and because they finely modulate the redox potential of DNA nucleobases, in a way which depends on the primary and higher order structures.[8] Indeed, there is experimental evidence that sequences of adjacent guanines (G), the nucleobase with the lowest oxidation potential, are the most easily oxidizable sites in DNA, with GGG sequences being still more reactive than GG ones.[9−19]

According to the simplest but physically well sound two-state quantum model, the hole energy levels of two stacked nucleobases are shifted up and down with respect to those of unstacked ones by a quantity related to the difference between the oxidation potentials of the two nucleobases and to the strength of the stacking interaction (β). Because of resonance, the effect is enhanced for equal nucleobases; in that case, the energy lowering amounts exactly to the interaction energy β (see Figure 1). The $\pi-\pi$ stacking interaction energy between two purines is expected to be in the range 0.1−0.3 eV for a neutral pair;[20,21] differential pulse voltammetry can easily detect oxidation potential differences of 0.1 V, providing a well suited experimental tool for detecting the presence of stacking interactions and determining their strengths in oxidized samples.[22] Here, we present a series of voltammetric measurements of oligonucleotides containing adenine (A) in different sequences and ratios, exhibiting multiple signals characteristic of π stacked molecular systems,[22] from which, upon a few reasonable assumptions, the π stacking interaction energy can be inferred.

EXPERIMENTAL AND COMPUTATIONAL DETAILS

All voltammetric measurements were performed at room temperature by using an Autolab PGSTAT302N potentiostat-galvanostat, using a positive feedback to compensate for ohmic drop. A standard three-electrode configuration was used, consisting of a glassy carbon disk (2 mm diameter) as a working electrode, a Pt bar as a counterelectrode, and a double junction Ag/AgCl (3 M KCl) electrode in which the outer compartment is filled with 0.10 M KCl in water. All the electrodes were purchased from Metrohm. All samples were deaerated before measurement. Oligonucleotides have been purchased from Sigma-Aldrich and used without further purification. Ultrapure water and phosphate buffer from Aldrich has been used throughout.

MD simulations were carried out at a constant temperature (300 K) by using the AMBER 11.0 suite of programs.[23] Starting geometries of single strands were generated from the A-DNA. K^+ counterions were added to neutralize the system and explicit solvent molecules have been included in simulations, by using the TIP3P solvent model.[24] The "solvateoct" command of LEaP was used to create a truncated octahedron box of water molecules surrounding the oligonucleotide with buffer distances of 8.0 Å between the walls of the box and the closest atoms of the solute. The initial dimensions of the periodic TIP3P water box were ca. 66000 Å^3, corresponding to 1734

Received: April 26, 2013
Revised: July 2, 2013

   dx.doi.org/10.1021/jp404133a | J. Phys. Chem. B XXXX, XXX, XXX−XXX

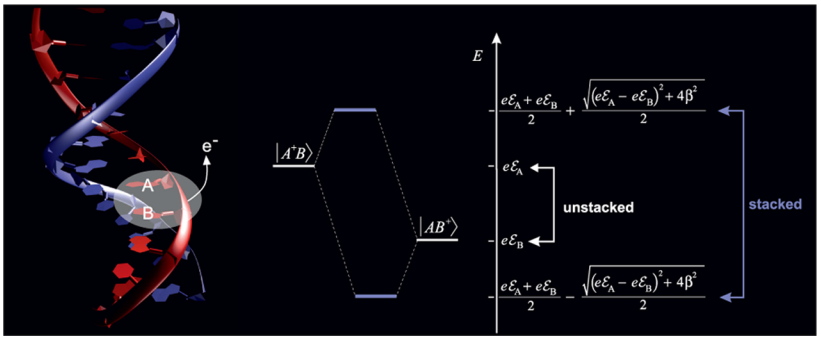

Figure 1. The effects of π stacking interactions upon the electronic states of one-electron-oxidized DNA: removal of an electron from an unstacked A and B nucleobase pair gives rise to two states $|A^+B\rangle$ and $|AB^+\rangle$, with energies $e\cdot\mathcal{E}_A$ and $e\cdot\mathcal{E}_B$, respectively (e = electron charge, $\mathcal{E}_{A/B}$ = oxidation potential); upon formation of a π stacking interaction, the two states are coupled with each other, and the energy levels of the electron hole are shifted up and down with respect to those of the unstacked pair by a factor depending on the strength of the π stacking interaction, β, and on the difference between nucleobase oxidation potentials, as shown on the right side of the panel.

water molecules. The SHAKE option was used for constraining bonds involving hydrogen atoms.

MD were performed at a constant pressure after a 20 ps period of constant volume equilibration heating the system from 0 to 300 K. The AMBER force field was used in all simulations.[25] Molecular dynamics were carried out on a 6 ns time scale. Conformations were sampled every 0.5 ps by using the PTRAJ module of the Amber package. A cutoff distance of 10 Å was used for Lennard-Jones interactions. The particle mesh Ewald (PME) method for the treatment of the long-range electrostatics was used with a distance cutoff of 10 Å.[26]

RESULTS

At the present stage of knowledge, we have preferred to start from short oligonucleotide sequences, hexamers, for which the assignments of the current/voltage signals to specific nucleobase sequences should not pose problems caused by the presence of overlapping signals, as could happen in natural DNA. The choice of starting from sequences containing A units is related to the highest ability of A of forming stacking interactions.[27] The examined sequences contain from two up to four adjacent A units, together with thymine (T) and cytosine (C) units, which, because of their higher oxidation potentials, should not interfere with A signals.

The differential pulse voltammetries of the palindromic sequences 5′-ACCCCA-3′ and 5′-AACCAA-3′, recorded at room temperature in 0.05 M phosphate buffer, are shown in Figure 2. While the 5′-ACCCCA-3′ sequence exhibits only one peak at ca. 1.24 V vs Ag/AgCl, 5′-AACCAA-3′ is characterized by two well resolved peaks, falling at 0.93 and 1.24 V. The former can be attributed to the oxidation of the pair of adjacent A's in a stacked nuclear configuration, and the other, very similar to that of 5′-ACCCCA-3′, is possibly due to the oxidation of the other A of the pair, on the condition that the first oxidation event has been followed by an irreversible reaction restoring the neutral charge on the oligonucleotide. The radical cation of A is expected to be a quite strong acid,[28] so that neutrality could be restored by removal of a proton from the exocyclic amine group of the oxidized A.

The interaction energy β, corresponding to the hole transfer probability amplitude between the two nucleobases, can be determined from the voltammograms of 5′-ACCCCA-3′ and 5′-AACCAA-3′, by making the reasonable assumption that standard potential differences are well approximated by peak potential ones and by neglecting the effects of the slightly

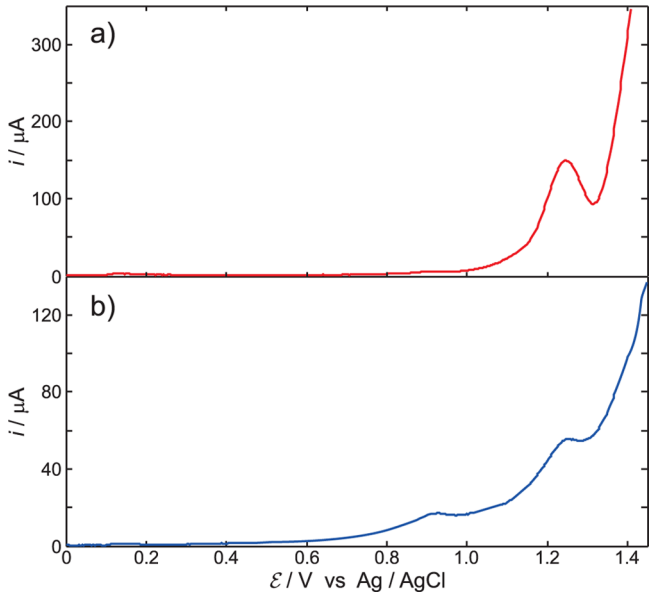

Figure 2. Differential pulse voltammetry of 2.0 mM 5′-ACCCCA-3′ (top) and 0.50 mM 5′-AACCAA-3′ (bottom) in 50 mM phosphate buffer solution; sweep rate 100 mV/s. Working electrode: glassy carbon disk, 2 mm. Internal reference electrode: double junction Ag/AgCl (3 M KCl) electrode in which the outer compartment is filled with 0.10 M KCl in water.

different environments experienced by the A pair of AACCAA and the single A unit in ACCCCA. In that case, the simple two-state model yields $|\beta|$ = 0.31 eV, the absolute value being used because the procedure used for estimating the coupling element does not provide information about the phase of the wave function. That value is of the same order of magnitude of those used for the hopping integrals between adjacent nucleotides (≈0.15−0.4 eV) for reproducing electron transport measurements,[29−32] but it is much higher than that obtained by *ab initio* calculations for B-DNA configurations;[33−36] see *infra*.

The above value has to be intended as an average over the possible conformational arrangements that the ending AA pair can assume; since the ending position of a hexamer is known to exhibit a higher conformational flexibility even in the solid state,[37] we have also considered other sequences, where the A pair is located in the central region of the hexamer.

The differential pulse voltammetries of the sequences 5′-TTAATT-3′, 5′-TTAAAT-3′, and 5′-TAAAAT-3′, recorded in

dx.doi.org/10.1021/jp404133a | J. Phys. Chem. B XXXX, XXX, XXX−XXX

the same conditions as the previous ones, are reported in Figure 3. As for 5′-AACCAA-3′, the voltammogram of 5′-TTAATT-3′

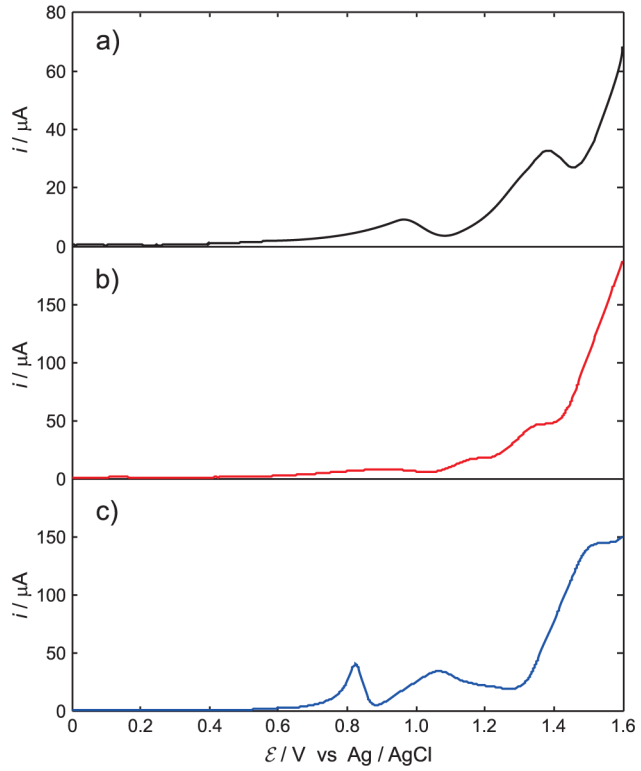

Figure 3. Differential pulse voltammetry of 0.50 mM 5′-TTAATT-3′ (a), 0.50 mM 5′-TTAAAT-3′ (b), and 1.0 mM 5′-TAAAAT-3′ (c) in 50 mM phosphate buffer solution. Scan rate and electrode arrangements as in Figure 2.

shows two peaks centered at 0.97 and 1.35 V. The first anodic peak can be safely assigned to oxidation of the two stacked A's; it falls at slightly higher potential (40 mV) than that of 5′-AACCAA-3′, possibly because of the lower solvent accessibility of the central zone of the oligonucleotide with respect to the ending one.[38] Although for the purposes of the present paper only the first oxidation peak is of interest, a few considerations on the possible assignment of the second peak can be of interest for stimulating further works. The second peak could be assigned to the oxidation of the second A units, as for 5′-AACCAA-3′, or alternatively to the oxidation of the two stacked thymines. Indeed, the latter possibility has to be taken into consideration especially in light of the finding that in oligonucleotides which lack G oxidative damages are mainly observed at T sites.[39,40] On the basis of that finding, it has been proposed that in duplex DNA T oxidation could possibly occur at potentials slightly higher (0.15 V) than A.[40] Noteworthy, a signal at 1.35 V is observed also in the 5′-TTAAAT-3′ oligonucleotide but not in 5′-TAAAAT-3′; see infra.

The voltammograms of 5′-TTAAAT-3′ and 5′-TAAAAT-3′ show that the first anodic signal falls at 0.90 V for the former sequence and at 0.82 V for the latter. Thus, a progressive lowering of the potential of the first anodic peak as the number of A bases increases is clearly observed, as already predicted by theoretical computations.[19]

The above results can be rationalized by using a simple effective tight-binding Hamiltonian:

$$\mathcal{H} = \sum_{n=1}^{L-1} \epsilon_n |n\rangle\langle n| + J_{n,n+1}(|n\rangle\langle n+1| + \text{H.c.}) + \epsilon_L |L\rangle\langle L| \quad (1)$$

where $|n\rangle$ represents the state with the hole localized on the nth nucleotide in the sequence, ϵ_n its energy, $J_{n,n+1}$ the coupling between $|n\rangle$ and $|n+1\rangle$ due to the stacking interaction between adjacent nucleobases, and L the number of nucleobase sites. The simple tight binding Hamiltonian of eq 1 has been widely employed for treating long-range charge transfer in DNA[29,35,36,41] and DNA hairpins.[42−44] For the 5′-TTAAAT-3′ sequence, the Hamiltonian matrix representation on the base of charge localized states is the familiar Hückel type matrix:

$$\mathbf{H} = \begin{pmatrix} e\mathcal{E}_T & J_{TT} & 0 & 0 & 0 & 0 \\ J_{TT} & e\mathcal{E}_T & J_{AT} & 0 & 0 & 0 \\ 0 & J_{AT} & e\mathcal{E}_A & J_{AA} & 0 & 0 \\ 0 & 0 & J_{AA} & e\mathcal{E}_A & J_{AA} & 0 \\ 0 & 0 & 0 & J_{AA} & e\mathcal{E}_A & J_{AT} \\ 0 & 0 & 0 & 0 & J_{AT} & e\mathcal{E}_T \end{pmatrix} \quad (2)$$

with $\mathcal{E}_i = \epsilon_i/e$, e being the electron charge, whose diagonalization yields hole energies.

In order to fix the parameters of the effective Hamiltonian, it is convenient to start from the palindromic 5′-TAAAAT-3′ sequence, for which, assuming full symmetry, only four parameters are needed: ϵ_A, ϵ_T, and the two charge transfer integrals J_{AA} and J_{AT}. From the voltammograms of Figure 2, we have set $|J_{AA}| = 0.31$ and $\epsilon_A = -1.25$ eV for the ending oligonucleotide position. For A in any internal position of the hexamer, the site energy is slightly decreased, $\epsilon_A = -1.35$ eV, in order to account for the lower solvent accessibility. Then, we set $\epsilon_T = \epsilon_A - 0.15$ eV, as suggested by recent studies on oxidative damages of oligonucleotides which lack guanine,[39,40] and $|J_{AT}| = 0.25$ eV, assuming that the latter is smaller than J_{AA}.[45] With the above parameters, the simple effective Hamiltonian of eq 1 predicts that for 5′-TAAAAT-3′ the highest energy hole state is at −0.82 eV, corresponding to the observed potential of the first anodic peak.

The choice of the parameters ϵ_T and J_{TA} does not affect significantly the energy of the highest hole state: roughly, a change by 20% of one parameter, keeping fixed the other, affects the highest hole energy by ca. 1%, for both ϵ_T and J_{TA}. Thus, the values $\epsilon_A = -1.35$ (inner position) and $|J_{AA}| = 0.31$ eV are robust enough for being used for the other sequences.

For 5′-TTAAAT-3′, the above parameters, together with $\epsilon_T = -1.60$ eV for the inner position (adopted just for coherence with the previous choice for A), predict that the highest hole state energy is −0.86 eV, independent of the $|J_{TT}|$ value in the range 0.0−0.3 eV. That value is well within the broad anodic signal observed in the voltammogram of 5′-TTAAAT-3′. Noteworthy, for 5′-TTAAAT-3′, molecular dynamics simulations, see infra, predict that the average stacking interaction between A_3 and A_4 is somewhat weaker than that for A_4−A_5, with a slight higher time average of the rise coordinate and a higher root-mean-square deviation; see Table 1. That would explain both the broadness of the first anodic peak, a weaker stacking interaction reflects into a larger conformational flexibility, and the slightly low hole energy predicted by the effective tight binding Hamiltonian; by increasing the charge

dx.doi.org/10.1021/jp404133a | J. Phys. Chem. B XXXX, XXX, XXX−XXX

Table 1. Averages and Root Mean Square Deviations (RMSDs) of the Rise (Å), Roll (deg), and Tilt (deg) Coordinates of Oligonucleotides from 6 ns Dynamics Simulations in Water

		rise		roll		tilt	
sequence	pair	av.	RMSD	av.	RMSD	av.	RMSD
TAAAAT	T_1A_2	0.83	2.4	54	121	−15	58
	A_2A_3	3.29	0.3	11	9	5	6
	A_3A_4	3.36	0.4	6	15	3	7
	A_4A_5	3.29	0.3	8	9	4	6
	A_5T_6	3.27	0.6	7	8	4	8
TTAAAT	A_3A_4	3.41	0.7	13	12	3	12
	A_4A_5	3.32	0.4	2	16	4	7
TTAATT	A_3A_4	3.32	0.4	6	13	4	6
AACCAA[a]	A_1A_2	3.33	0.4	9	12	4	7
	C_3C_4	5.51	3	27	20	−22	38
	A_3A_6	3.34	0.6	12	11	4	9

[a]From a 3.5 ns MD simulation.

transfer integral for the A_3-A_4 pair to −0.25 eV, the hole energy rises to −0.90 eV, corresponding to the potential at which the broad anodic signal is centered. Keeping now fixed all the parameters, the effective tight binding Hamiltonian predicts that for 5′-TTAATT-3′ the energy of the highest hole state is −0.94 eV, slightly higher (30 meV) than the observed one. We remark that the above analysis refers to a coarse grained description of the average hexamer conformations; a full symmetrical arrangement has been assumed in setting the parameters, while molecular dynamics simulations, although grossly confirming that picture, suggest that some sites in the hexamers experience a greater rigidity than others; see infra.

All the voltammetric measurements reported here point toward the formation in solution of well structured oligonucleotide conformations. That finding has been tested by performing molecular dynamics (MD) simulations for all the analyzed oligonucleotides.

Even starting from geometries generated from the A-DNA form, the single strands quickly assume conformations of the B-DNA type, which are roughly maintained for all the simulation time. A few test simulations, carried out only for the 5′-TAAAAT-3′ sequence, starting with completely random strand conformations have also been performed (see infra).

The results have been analyzed in terms of the rise, tilt, and roll coordinates, the most suited ones for analyzing intrastrand stacking interactions.[46] The rise coordinate measures the displacement along the helix axis of a nucleobase with respect to its predecessor (3.32−3.36 Å for the B-DNA form), whereas the tilt and roll coordinates (0° for B-DNA) measure the relative inclination of a nucleobase plane relative to its predecessor.

The time evolution of the five rise coordinates of the 5′-TAAAAT-3′ sequence is shown in Figure 4; average values and root-mean-square deviations of the whole set of the three coordinates for 5′-TAAAAT-3′ and of those concerning A nucleobases for the other sequences studied here are reported in Table 1.

For the 5′-TAAAAT-3′ sequence, MD simulations indicate a well structured conformation in solution. All the rise coordinates are very similar to that characteristic of the B-DNA form but for that concerning the first step 5′-T-A-3′, which, as expected, possesses a much higher flexibility, as exhibited even in the solid state.[37] The same also occurs for

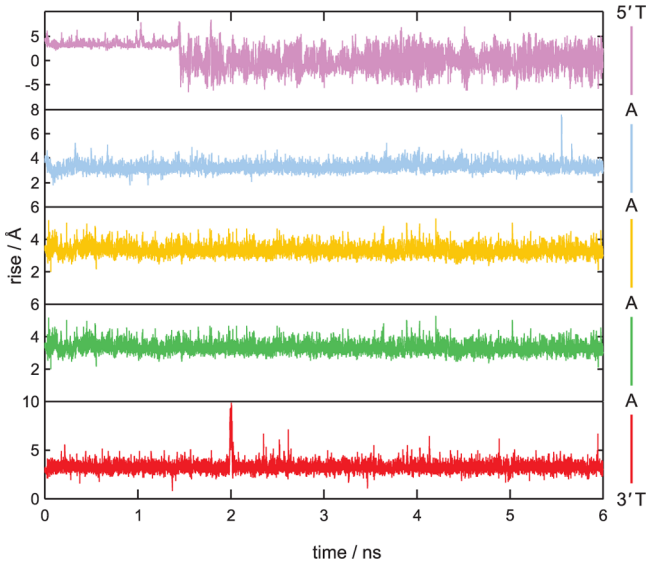

Figure 4. Time evolution of the five rise coordinates of 5′-TAAAAT-3′, starting from the 5′-TA pair (top) up to the AT-3′ one (bottom), during 6 ns dynamics simulations in water.

both the roll and tilt coordinates, which are restricted within a few degrees but for the first 5′-TA step. A few test computations have been performed only for the 5′-TAAAAT-3′ sequence, starting from completely random conformations of the strand and using a 12 ns time scale. No significant changes have been observed on the nanosecond time scale; the strand employs ∼3−4 ns to achieve a B-DNA form, which is roughly maintained for the remaining 9 ns, but for the A_2-A_3 step which exhibits a much higher flexibility of all the others. Thus, MD simulations provide a full support to the results of voltammetric measurements: the four A nucleobases appear to be well stacked with each other, as the shift at lower potential of the first voltammetric signal has led to suppose. A snapshot of the strand, on average well representative of the time dynamics, is shown in Figure 5.

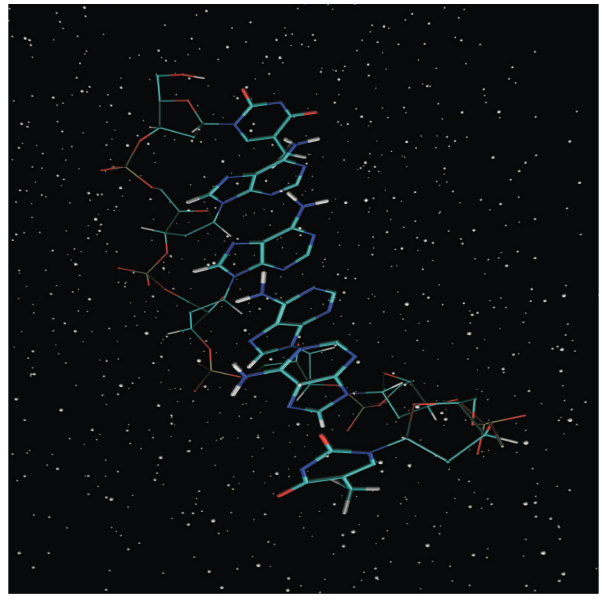

Figure 5. Snapshot of a well representative structure of 5′-TAAAAT-3′ from dynamic trajectories. Water molecules are depicted as white dots.

dx.doi.org/10.1021/jp404133a | J. Phys. Chem. B XXXX, XXX, XXX−XXX

For the 5′-TTAAAT-3′ sequence, MD simulations yield similar results: the three A units are on average well stacked with each other, even though the average rise coordinate for the A_3A_4 pair is slightly longer with a much greater RMS deviation. That is an indication of a higher conformational flexibility, which, as discussed above, explains the broadness of the observed voltammetric signal; see Figure 3b. Similar results also hold for 5′-TTAATT-3′; the two A's are well stacked with each other; the average rise coordinate is 3.32 Å; and the tilt and roll are 4 and 6°, respectively.

As concerns 5′-AACCAA-3′, MD simulations predict that its time average conformation consists of two weakly interacting blocks of three well stacked nucleobases (AAC). Indeed, the rise coordinates concerning the two ending AA pair are 3.33 and 3.34 Å, whereas that for the C_3C_4 pair is 5.51 Å. A representative snapshot of the molecular structure is shown in Figure 6.

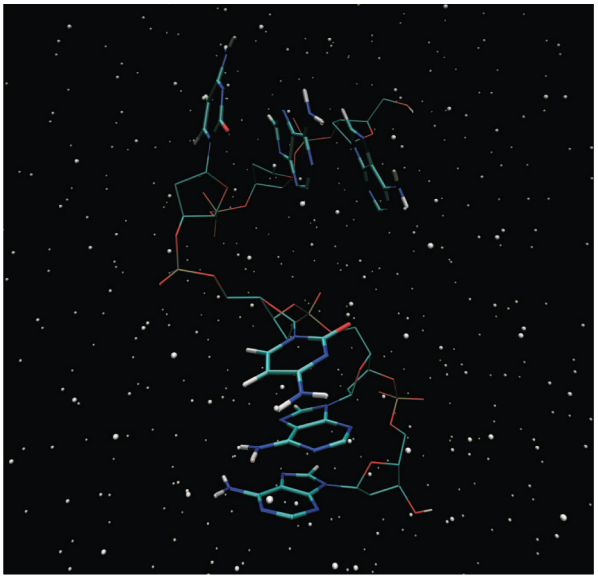

Figure 6. Snapshot of a well representative structure of 5′-AACCAA-3′ from dynamic trajectories.

DISCUSSION

DPV measurements have shown that stacking interactions in resonance conditions (between homobases) significantly lower the oxidation potential of sequences containing up to four consecutive adenines. That result is somewhat intriguing inasmuch one could be induced to argue that in duplex DNA a hole could preferentially localize on a sequence of stacked A's rather than on G units.[47] Although in principle possible, and indeed oxidative damages at A sites exhibit the second highest score in duplex DNA, that is however unlikely. First of all, the lowering of the oxidation potential of G by hydrogen bonding with its complementary base C is larger than that observed for the pairing of A with T. Voltammetric measurements carried out in non-protic solvents, where the effects of the complementary base pairing is included, have shown that the current/potential peak of the Watson−Crick G:C complex falls at 0.57 V vs Fc^+/Fc,[48] whereas the H-bond complex between A and T exhibits a peak at 1.0 V vs Fc/Fc^+.[49] The peak difference observed in voltammetric measurements is 0.43 V, which is high enough to make an isolated G competitive with a sequence of four stacked A's, especially in duplex DNA where the oxidation potential of a single G unit will also be affected by stacking interactions with the adjacent bases, which, even though in off-resonance conditions (heterobase), can easily provide further stabilization energy.

Another point which deserves some attention concerns the interpretative model we have used. Here we have chosen a set of base states corresponding to the charge completely localized on a single nucleobase. That choice is mandatory for keeping as low as possible the numbers of unknowns which have to be inferred from experimental data. Within that scheme, hole energies depend only on the nucleobase on which the hole is localized and are rigorously independent of nucleobase sequence, so that the large shifts in the oxidation potentials of sequences containing consecutive A's are fully attributed to the electronic coupling. Because of that, the hole hopping parameter between two stacked A units comes out to be larger than that estimated by electronic wave function calculations[33−36] but of the same order of magnitude of those used for the hopping integrals between adjacent nucleotides (≈0.15−0.4 eV) for reproducing electron transport measurements.[29−32] While our choice of the diabatic states seems to be the same as that adopted in ref 33, where the hole hopping parameter for equivalent donor and acceptor was estimated as half of the splitting between adiabatic states, computed in the frame of Koopmans' approximation, it is however different from that used in ref 36, where hole site energies which depend on the base sequence are considered. In the latter approach, the adopted diabatic states are different from those considered here, so that a direct comparison is not possible. Noteworthy, by using the hole site energies and the coupling parameters adopted above, i.e., $\epsilon_A = -1.35$, $\epsilon_T = -1.60$, $|J_{AA}| = 0.31$, and $|J_{AT}| = 0.25$ eV, the tight binding Hamiltonian predicts that the hole site energies of AAA and TAT are −0.91 and −1.11 eV, respectively, with a shift of 0.2 eV, which is even smaller than that reported in ref 36.

CONCLUSIONS

In one-electron-oxidized oligonucleotides intrastrand stacking interactions give rise to a complex distribution of low lying electronic states, because the four nucleobases have different oxidation potentials, varying in the range of about 1 V,[50] which in turn are significantly modulated by nonbonding interbase interactions—hydrogen bonds[48,49] and π stacking[10,11]—in a way which depends on the primary and higher order DNA structures.[8] Here, we have shown that differential pulse voltammetry is a powerful method to investigate how hole site energies depend on the specific nucleobase sequence in short oligonucleotides, providing useful information for understanding the complex landscape of the excited electronic states in oxidized DNA, which in turn controls long-range hole transfer.

AUTHOR INFORMATION

Corresponding Author

*E-mail: apeluso@unisa.it.

Notes

The authors declare no competing financial interest.

ACKNOWLEDGMENTS

The financial support of MIUR (PRIN09) is gratefully acknowledged.

REFERENCES

(1) Murphy, C. J.; Arkin, M. R.; Jenkins, Y.; Ghatlia, N. D.; Bossmann, S. H.; Turro, N. J.; Barton, J. K. Long-Range Photoinduced Electron Transfer through a DNA Helix. *Science* **1994**, *262*, 1025−1029.

(2) Murphy, C. J.; Arkin, M. R.; Ghatlia, N. D.; Bossmann, S. H.; Turro, N. J.; Barton, J. K. Fast Photoinduced Electron Transfer through DNA Intercalation. *Proc. Natl. Acad. Sci. U.S.A.* **1994**, *91*, 5315−5319.

(3) Schuster, G. B. Long-Range Charge Transfer in DNA: Transient Structural Distortions Control the Distance Dependence. *Acc. Chem. Res.* **2000**, *33*, 253−260.

(4) Giese, B. Long Distance Charge Transport in DNA: the Hopping Mechanism. *Acc. Chem. Res.* **2000**, *33*, 631−636.

(5) Giese, B.; Amaudrut, J.; Köhler, A.-K.; Spormann, M.; Wessely, S. Direct Observation of Hole Transfer through DNA by Hopping between Adenine Bases and by Tunneling. *Nature* **2001**, *412*, 318−320.

(6) Takada, T.; Kawai, K.; Fujitsuka, M.; Majima, T. Direct Observation of Hole Transfer through Double Helical DNA over 100 Å. *Proc. Natl. Acad. Sci. U.S.A.* **2004**, *101*, 14002−14006.

(7) Genereux, J. C.; Barton, J. K. Mechanisms for DNA Charge Transport. *Chem. Rev.* **2010**, *110*, 1642−1662.

(8) Kanvah, S.; Joseph, J.; Schuster, G. B.; Barnett, R. N.; Cleveland, C. L.; Landman, U. Oxidation of DNA: Damage to Nucleobases. *Acc. Chem. Res.* **2009**, *43*, 280−287.

(9) Kovalsky, O. I.; Panyutin, I. G.; Budowsky, E. I. Sequence-Specificity of Alkali-Sensitive Lesions Induced in DNA by High-Intensity Ultraviolet Laser Radiation. *Photochem. Photobiol.* **1990**, *52*, 509−517.

(10) Saito, I.; Takayama, M.; Sugiyama, H.; Nakatani, K.; Tsuchida, A.; Yamamoto, M. Photoinduced DNA Cleavage via Electron Transfer: Demonstration That Guanine Residues Located 5′ to Guanine Are the Most Electron-Donating Sites. *J. Am. Chem. Soc.* **1995**, *117*, 6406−6407.

(11) Sugiyama, H.; Saito, I. Theoretical Studies of GG-Specific Photocleavage of DNA via Electron Transfer: Significant Lowering of Ionization Potential and 5′-Localization of HOMO of Stacked GG Bases in B-Form DNA. *J. Am. Chem. Soc.* **1996**, *118*, 7063−7068.

(12) Muller, J. G.; Hickerson, R. P.; Perez, R. J.; Burrows, C. J. DNA Damage from Sulfite Autoxidation Catalyzed by a Nickel(II) Peptide. *J. Am. Chem. Soc.* **1997**, *119*, 1501−1506.

(13) Nakatani, K.; Fujisawa, K.; Dohno, C.; Nakamura, T.; Saito, I. p-Cyano Substituted 5-Benzoyldeoxyuridine as a Novel Electron-Accepting Nucleobase for One-Electron Oxidation of DNA. *Tetrahedron Lett.* **1998**, *39*, 5995−5998.

(14) Yoshioka, Y.; Kitagawa, Y.; Takano, Y.; Yamaguchi, K.; Nakamura, T.; Saito, I. Experimental and Theoretical Studies on the Selectivity of GGG Triplets toward One-Electron Oxidation in B-Form DNA. *J. Am. Chem. Soc.* **1999**, *121*, 8712−8719.

(15) Hickerson, R. P.; Prat, F.; Muller, J. G.; Foote, C. S.; Burrows, C. J. Sequence and Stacking Dependence of 8-Oxoguanine Oxidation: Comparison of One-Electron vs Singlet Oxygen Mechanisms. *J. Am. Chem. Soc.* **1999**, *121*, 9423−9428.

(16) Nakatani, K.; Dohno, C.; Saito, I. Modulation of DNA-Mediated Hole-Transport Efficiency by Changing Superexchange Electronic Interaction. *J. Am. Chem. Soc.* **2000**, *122*, 5893−5894.

(17) Giese, B.; Wessely, S. The Influence of Mismatches on Long-Distance Charge Transport through DNA. *Angew. Chem., Int. Ed.* **2000**, *39*, 3490−3494.

(18) Kumar, A.; Sevilla, M. D. Photoexcitation of Dinucleoside Radical Cations: A Time-Dependent Density Functional Study. *J. Phys. Chem. B* **2006**, *110*, 24181−24188.

(19) Kumar, A.; Sevilla, M. D. Density Functional Theory Studies of the Extent of Hole Delocalization in One-Electron Oxidized Adenine and Guanine Base Stacks. *J. Phys. Chem. B* **2011**, *115*, 4990−5000.

(20) Ke, C.; Humeniuk, M.; S-Gracz, H.; Marszalek, P. E. Direct Measurements of Base Stacking Interactions in DNA by Single-Molecule Atomic-Force Spectroscopy. *Phys. Rev. Lett.* **2007**, *99*, 018302-4.

(21) Cysewski, P.; Czyżnikowska, Z.; Zaleśny, R.; Czeleń, P. The Post-SCF Quantum Chemistry Characteristics of the Guanine−Guanine Stacking in B-DNA. *Phys. Chem. Chem. Phys.* **2008**, *10*, 2665−2672.

(22) Qi, H.; Chang, J.; Abdelwahed, S. H.; Thakur, K.; Rathore, R.; Bard, A. J. Electrochemistry and Electrogenerated Chemiluminescence of π-Stacked Poly(fluorenemethylene) Oligomers. Multiple, Interacting Electron Transfers. *J. Am. Chem. Soc.* **2012**, *134*, 16265−16274.

(23) Case, D. A. et al. *AMBER 11*; University of California: San Francisco, CA, 2011.

(24) Price, D. J.; Brooks, C. L. A Modified TIP3P Water Potential for Simulation with Ewald Summation. *J. Chem. Phys.* **2004**, *121*, 10096−10103.

(25) Cheatham, T. E., III; Cieplak, P.; Kollman, P. A. A Modified Version of the Cornell et al. Force Field with Improved Sugar Pucker Phases and Helical Repeat. *J. Biomol. Struct. Dyn.* **1999**, *16*, 845−862.

(26) Toukmaji, A.; Sagui, C.; Board, J.; Darden, T. Efficient Particle-Mesh Ewald Based Approach to Fixed and Induced Dipolar Interactions. *J. Chem. Phys.* **2000**, *113*, 10913−10927.

(27) Czyżnikowska, Ż.; Zaleśny, R.; Papadopoulos, M. G. In *Practical Aspects of Computational Chemistry: Methods, Concepts and Applications*, 57th ed.; Leszczyński, J., Shukla, M. K., Eds.; European Academy of Sciences, Springer: The Netherlands, 2009; p 392.

(28) Candeias, L. P.; Steenken, S. Ionization of Purine Nucleosides and Nucleotides and Their Components by 193-nm Laser Photolysis in Aqueous Solution: Model Studies for Oxidative Damage of DNA. *J. Am. Chem. Soc.* **1992**, *114*, 699−704.

(29) Roche, S. Sequence Dependent DNA-Mediated Conduction. *Phys. Rev. Lett.* **2003**, *91*, 108101−108104.

(30) Cuniberti, G.; Craco, L.; Porath, D.; Dekker, C. Backbone-Induced Semiconducting Behavior in Short DNA Wires. *Phys. Rev. B* **2002**, *65*, 241314-4.

(31) Porath, D.; Bezryadin, A.; de Vries, S.; Dekker, C. Direct Measurements of Electrical Transport Through DNA Molecules. *Nature* **2000**, *403*, 635−638.

(32) Conwell, E. M.; Rakhamanova, S. V. Polarons in DNA. *Proc. Natl. Acad. Sci. U.S.A.* **2000**, *97*, 4556−4560.

(33) Voityuk, A. A.; Jortner, J.; Bixon, M.; Rösch, N. Electronic Coupling between Watson-Crick Pairs for Hole Transfer and Transport in Desoxyribonlucleic Acid. *J. Chem. Phys.* **2001**, *114*, 5614−5620.

(34) Troisi, A.; Orlandi, G. Hole Migration in DNA: a Theoretical Analysis of the Role of Structural Fluctuations. *J. Phys. Chem. B* **2002**, *106*, 2093−2101.

(35) Senthilkumar, K.; Grozema, F. C.; Fonseca Guerra, C.; Bickelhaupt, F. M.; Siebbeles, L. D. A. Mapping the Sites for Selective Oxidation of Guanines in DNA. *J. Am. Chem. Soc.* **2003**, *125*, 13658−13659.

(36) Senthilkumar, K.; Grozema, F. C.; Fonseca Guerra, C.; Bickelhaupt, F. M.; Lewis, F. D.; Berlin, Y. A.; Ratner, M. A.; Siebbeles, L. D. A. Absolute Rates of Hole Transfer in DNA. *J. Am. Chem. Soc.* **2005**, *127*, 14894−14903.

(37) Abrescia, N. G. A.; González, C.; Gouyette, C.; Subirana, J. A. X-ray and NMR Studies of the DNA Oligomer d(ATATAT): Hoogsteen Base Pairing in Duplex DNA. *Biochemistry* **2004**, *43*, 4092−4100.

(38) Sistare, M. F.; Codden, S. J.; Heimlich, G.; Thorp, H. H. Effects of Base Stacking on Guanine Electron Transfer: Rate Constants for G and GG Sequences of Oligonucleotides from Catalytic Electrochemistry. *J. Am. Chem. Soc.* **2000**, *122*, 4742−4749.

(39) Abraham, J.; Gosh, A. K.; Schuster, G. B. One-Electron Oxidation of DNA Oligomers That Lack Guanine: Reaction and Strand Cleavage at Remote Thymines by Long-Distance Radical Cation Hopping. *J. Am. Chem. Soc.* **2006**, *128*, 5346−5347.

(40) Barnett, R. N.; Joseph, J.; Landman, U.; Schuster, G. B. Oxidative Thymine Mutation in DNA: Water-Wire-Mediated Proton-Coupled Electron Transfer. *J. Am. Chem. Soc.* **2013**, *135*, 3904−3914.

(41) Schuster, G. B. Long-Range Charge Transfer in DNA. II. *Top. Curr. Chem.* **2004**, 237.
(42) Tuma, J.; Tonzani, S.; Schatz, G. C.; Karaba, A. H.; Lewis, F. D. Structure and Electronic Spectra of DNA Mini-Hairpins with Gn:Cn Stems. *J. Phys. Chem. B* **2007**, *111*, 13101−13106.
(43) Grozema, F. C.; Tonzani, S.; Berlin, Y. A.; Schatz, G. C.; Siebbeles, L. D. A.; Ratner, M. A. Effect of Structural Dynamics on Charge Transfer in DNA Hairpins. *J. Am. Chem. Soc.* **2008**, *130*, 5157−5166.
(44) Grozema, F. C.; Tonzani, S.; Berlin, Y. A.; Schatz, G. C.; Siebbeles, L. D. A.; Ratner, M. A. Effect of GC Base Pairs on Charge Transfer through DNA Hairpins: The Importance of Electrostatic Interactions. *J. Am. Chem. Soc.* **2009**, *131*, 14204−14205.
(45) Broom, A. D.; Schweizer, M. P.; Ts'O, P. O. P. Interaction and Association of Bases and Nucleosides in Aqueous Solutions. V. Study of the Association of Purine Nucleosides by Vapor Pression Osmometry and by Proton Magnetic Resonance. *J. Am. Chem. Soc.* **1967**, *89*, 3612−3622.
(46) Dickerson, R. E. Definitions and Nomenclature of Nucleic Acid Structure Components. *Nucleic Acids Res.* **1989**, *17*, 1797−1803.
(47) We are indebted to reviewers for having drawn that point to our attention.
(48) Caruso, T.; Carotenuto, M.; Vasca, E.; Peluso, A. Direct Experimental Observation of the Effect of the Base Pairing on the Oxidation Potential of Guanine. *J. Am. Chem. Soc.* **2005**, *127*, 15040−15041.
(49) Caruso, T.; Capobianco, A.; Peluso, A. The Oxidation Potential of Adenosine and Adenosine-Thymidine Base-Pair in Chloroform Solution. *J. Am. Chem. Soc.* **2007**, *129*, 15347−15353.
(50) Capobianco, A.; Carotenuto, M.; Caruso, T.; Peluso, A. The Charge-Transfer Band of an Oxidized Watson-Crick Guanosine-Cytidine Complex. *Angew. Chem., Int. Ed.* **2009**, *48*, 9526−9528.